Science Translational Medicine
AAAS

Supplementary Materials for

Sphingosine 1-phosphate signaling in perivascular cells enhances inflammation and fibrosis in the kidney

Shinji Tanaka *et al.*

Corresponding author: Mark D. Okusa, mdo7y@virginia.edu

Sci. Transl. Med. **14**, eabj2681 (2022)
DOI: 10.1126/scitranslmed.abj2681

The PDF file includes:

Other Supplementary Material for this manuscript includes the following:

Materials and methods

Assessment of kidney function and histology

Plasma was prepared by centrifuging heparinized blood at 7,000 g for 5 min. Plasma creatinine concentration were determined by using an enzymatic method as per the manufacturer's protocol (Diazyme Laboratories) that we have validated using liquid chromatograph-mass spectrometry (*70*). Blood urea nitrogen (BUN) concentrations were measured using the DetectX Urea Nitrogen (BUN) Detection kit (Arbor Assays). Collagen, the most abundant extracellular matrix protein, was detected using Masson's trichrome stain (*27*) and picrosirius red stain with polarized microscopy. Picrosirus red staining and quantification was performed as previously described (*68*). Briefly, photomicrographs of picrosirius red birefringence were captured by light microscopy with a polarizing filter (Zeiss AxioImager Z1 microscope, Carl Zeiss Microscopy) at 200X using Stereo Investigator software (Version 11; MBF Bioscience). Quantification of the fibrotic area was done by averaging total red/yellow birefringent pixels of ten random cortex fields per kidney section with ImageJ software. The extent of AKI was assessed with hematoxylin and eosin (H&E)-stained kidney sections in an unbiased, systematic manner using design-based stereology to achieve statistically accurate random sampling of kidney sections, yielding the percentage of total area of the section occupied by injured tubules (identified based on the presence of cast formation, tubule dilation, and/or tubular epithelial denucleation) as previously described (*70*). Plasma creatinine and BUN measurements and histological evaluation were performed by investigators blinded to the experimental setting.

Genotyping, quantitative real-time PCR, and Western blotting

For genotyping, DNA from kidneys and cells was isolated using Dneasy Blood & Tissue Kit (Qiagen). Bone marrow cells were isolated as previously described (*71*). mRNA from kidneys and cells was isolated by following the ethanol-precipitation method and using RNeasy Mini Kit (Qiagen), respectively. RNA concentration was determined based on spectrophotometric determination of a 260/280 ratio. cDNA was generated from the resultant tissue RNA using the iScript cDNA Synthesis Kit (Bio-Rad). Resultant cDNA

was then used to determine relative mRNA expression using the iTAC Universal SYBR Green Supermix (Bio-Rad). Primer sequences for genotyping and quantitative real-time PCR are shown in **Table S1**. Western blotting (40 μg protein) was performed as previously described (*69*). The following antibodies were used: a rabbit polyclonal anti-SphK2 antibody (1:1,000; #17096-1-AP; Proteintech), a rabbit polyclonal anti-SphK1 antibody (1:200; #10670-1-AP; Proteintech), a rabbit monoclonal anti-α-smooth muscle actin antibody (1:30,000; #ab124964; Abcam), and a mouse monoclonal anti-β-actin antibody (1:15,000; #ab6276; Abcam).

Flow cytometry

Immune cells in peripheral blood, spleen and inguinal lymph nodes were analyzed by flow cytometry. To make a single cell suspension, spleen and inguinal lymph nodes were weighed and teased through a 40-μm cell strainer (Thermo Fisher Scientific) via the rubber end of a 5-ml syringe plunger and then centrifuged at 500 g for 5 minutes at 4°C. For peripheral blood and spleen, red blood cells were lysed with red blood cell lysis buffer (BioLegend) as per the manufacturer's protocol. The cells were resuspended with 0.5% bovine serum albumin (BSA) in phosphate-buffered saline (PBS). After blocking nonspecific Fc binding with anti-mouse CD16/32 (2.4G2), cell suspensions were incubated with the following antibodies: anti-mouse CD3e-APC–eFluor 780 (145-2C11, Thermo Fisher Scientific), CD4-eFluor 660 (GK1.5, Thermo Fisher Scientific), CD8a-Alexa Fluor 488 (53-6.7, Thermo Fisher Scientific), CD19-PE–Cyanine7 (eBio1D3, Thermo Fisher Scientific) (for gating lymphocytes); F4/80-Alexa Fluor 488 (BM8, Thermo Fisher Scientific), CD115-APC (AFS98, Thermo Fisher Scientific), CD11b-PE–Cyanine7 (M1/70, BioLegend) (for gating macrophages and monocytes); CD45-Brilliant Violet 510 (30-F11, BioLegend) (for gating lymphocytes, macrophages and monocytes). 7-aminoactinomycin D (7-AAD, Thermo Fisher Scientific) was used to exclude dead cells. Counting Beads (CountBright Absolute Counting Beads, Thermo Fisher Scientific) were used to calculate the cell number. For compensation, compensation beads (UltraComp eBeads, Thermo Fisher Scientific) were used. Flow cytometry data were acquired on a BD FACSCalibur (BD Biosciences) with Cytek 8 Color Flow Cytometry Upgrade (Cytek Development Inc.) and analyzed by FlowJo software 10.7.1 (FlowJo Inc.).

S1P measurement (primary kidney perivascular cell, medium, plasma)

Primary kidney perivascular cells were washed with PBS and incubated for 6 hours with FBS-free medium containing 0.5% fatty acid-free BSA with SLM6031434 (SphK2 inhibitor), SLF1081851 (Spns2 inhibitor) or vehicle (0.1% fatty acid-free BSA). Protein (with S1P bound) was recovered from culture medium by ammonium sulfate precipitation, and the samples were prepared for LC-MS analysis as described previously (*30*). Cell pellets were processed as described previously for LC-MS analysis (*30*). Plasma was prepared and S1P was extracted for LC-MS analysis as reported previously (*30*).

Immunofluorescence

For immunofluorescent labeling of kidney sections, samples were prepared and analyzed as previously described (*68*). Periodate-lysine-paraformaldehyde-fixed frozen sections were stained with an anti-PDGFRβ (goat polyclonal, 1:600; AF1042; R&D Systems), anti-CD31 (goat polyclonal, 1:150; AF3628; R&D Systems) or anti-F4/80 antibody (rat monoclonal, 1:800; Clone Cl:A3-1; Bio-Rad) followed by Cy3-tagged anti-goat IgG (1:500, Jackson ImmunoResearch) or Alexa Fluor 555-tagged anti-rat IgG (1:600, Thermo Fisher Scientific). Quantification of F4/80 positive area was done by averaging total F4/80 positive pixels of ten random cortex fields (at 200X) per kidney section with ImageJ software.

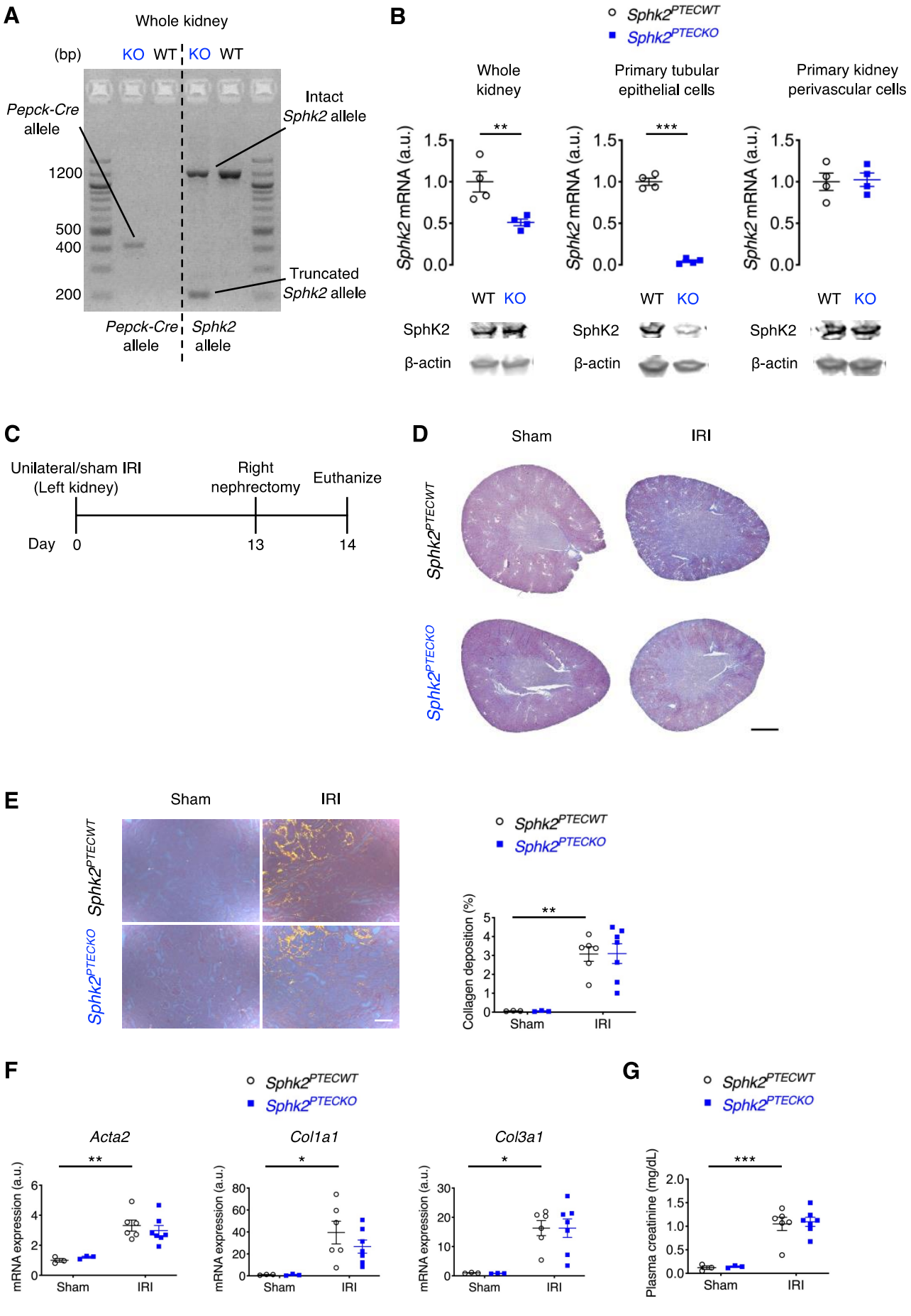
A
Whole kidney
(bp)
KO WT KO WT
Pepck-Cre allele
Intact Sphk2 allele
1200
500
400
200
Truncated Sphk2 allele
Pepck-Cre allele
Sphk2 allele
B
Sphk2PTECWT
Sphk2PTECKO
Whole kidney
Primary tubular epithelial cells
Primary kidney perivascular cells
Sphk2 mRNA (a.u.)
**
***
WT KO
SphK2
β-actin
C
Unilateral/sham IRI (Left kidney)
Right nephrectomy
Euthanize
Day 0
13
14
D
Sham
IRI
Sphk2PTECWT
Sphk2PTECKO
E
Sham
IRI
Sphk2PTECWT
Sphk2PTECKO
Collagen deposition (%)
**
Sham
IRI
F
Sphk2PTECWT
Sphk2PTECKO
Acta2
Col1a1
Col3a1
mRNA expression (a.u.)
**
*
*
Sham
IRI
G
Sphk2PTECWT
Sphk2PTECKO
Plasma creatinine (mg/dL)
***
Sham
IRI

Figure S1. *Sphk2* in proximal tubular epithelial cells does not play an important role in the progression of kidney fibrosis. (**A** and **B**) Validation of *Sphk2*^{PTECKO} mice (*Pepck-Cre;Sphk2*$^{fl/fl}$ mice), in which *Sphk2* is deleted in renal proximal tubular epithelial cells. (**A**) Genotyping of *Pepck-Cre* and floxed *Sphk2* alleles. Agarose gel analysis of PCR products amplified from the DNA isolated from whole kidneys of *Sphk2*^{PTECKO} mice (KO) and Cre-negative littermate control mice (*Sphk2*^{PTECWT}, WT). Intact *Sphk2* allele = 1220 bp, truncated *Sphk2* allele = 203 bp (cut by Cre recombinase), *Pepck-Cre* allele = 411 bp. (**B**) *SphK2* expression in primary tubular epithelial cells (mostly proximal tubular epithelial cells) and primary perivascular cells (pericytes and fibroblasts) isolated from the kidneys of *Sphk2*^{PTECWT} (WT) and *Sphk2*^{PTECKO} (KO) mice, and in the whole kidneys of those mice. (**C** to **G**) No differences in kidney fibrosis in *Sphk2*^{PTECWT} and *Sphk2*^{PTECKO} mice after unilateral ischemia-reperfusion injury (IRI). (**C**) Protocol for unilateral IRI (for **D** to **G**). *Sphk2*^{PTECWT} and *Sphk2*^{PTECKO} mice underwent left renal pedicle clamp for 26 min (day 0) and right nephrectomy at day 13, and were euthanized at day 14. (**D**) Representative Masson's trichrome staining of collagen in kidney sections at day 14. (**E**) Picrosirius red staining of kidney (polarized microscopy) with quantification of red/yellow birefringence of mature collagen fibers as a percentage of the total surface area of kidney section at day 14. (**F**) *Acta2*, *Col1a1*, and *Col3a1* transcript expression (from whole kidney) at day 14. (**G**) Plasma creatinine concentrations at day 14. Scale bars: 1 mm (**D**) and 200 μm (**E**). $n = 4$ per group (**B**), $n = 3$-7 per group (**C**-**G**). Data are represented as mean ± SEM. *$P < 0.05$, **$P < 0.01$, ***$P < 0.001$; unpaired two-sided Student's *t* test (**B**), two-way ANOVA followed by post hoc multiple-comparison test (Tukey's) (**E** to **G**).

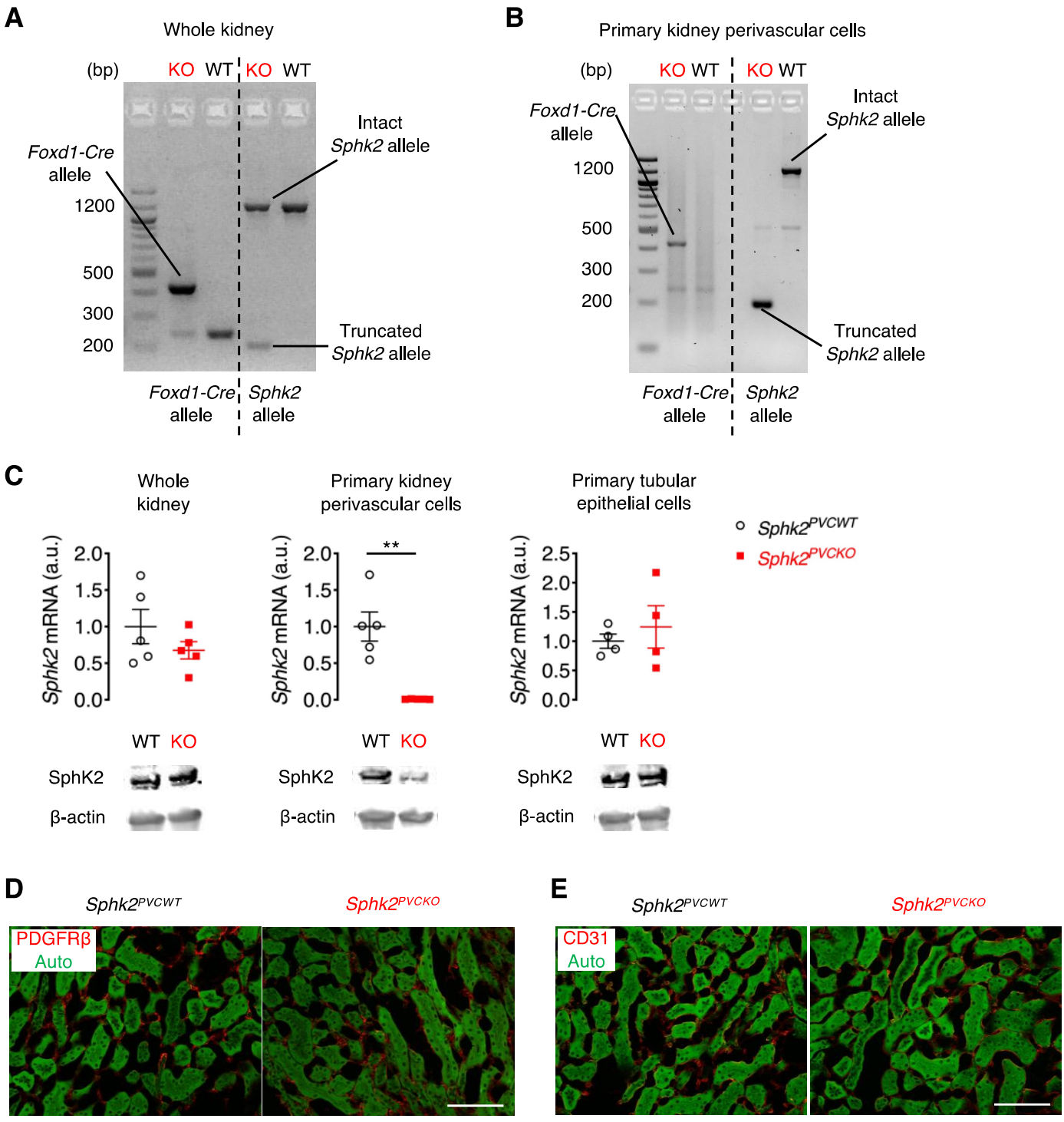

Figure S2. Validation of *Sphk2*^{PVCKO} mice. (**A** and **B**) Genotyping of *Foxd1-Cre* and floxed *Sphk2* alleles. Agarose gel analysis of PCR products amplified from the DNA isolated from whole kidneys (**A**) and primary kidney perivascular cells (**B**) of *Foxd1-Cre;Sphk2*$^{fl/fl}$ mice (*Sphk2*^{PVCKO}, KO), in which *Sphk2* is deleted in kidney perivascular cells, and Cre-negative littermate control mice (*Sphk2*^{PVCWT}, WT). Intact *Sphk2* allele = 1220 bp, truncated *Sphk2* allele = 203 bp (cut by Cre recombinase), *Foxd1-Cre* allele = 450 bp. Note that

whole kidneys contain both Foxd1-lineage and non-Foxd1-lineage cells (**A**) whereas WT and KO kidney perivascular cells have only intact and truncated *Sphk2* allele, respectively (**B**), indicating a high efficiency of Cre recombination, which is consistent with a previous report [about 100% in PDGFRβ-positive cells (*29*)], and a high purity of the primary kidney perivascular cells. (**C**) *SphK2* expression in the primary perivascular cells (pericytes/fibroblasts) and primary tubular epithelial cells isolated from the kidneys of $Sphk2^{PVCWT}$ (WT) and $Sphk2^{PVCKO}$ (KO) mice and in the whole kidneys of those mice. n = 4-5 per group. Data are represented as mean ± SEM. $^{**}P < 0.01$; unpaired two-sided Student's t test. (**D** and **E**) Unaltered vascular patterning in the kidney of $Sphk2^{PVCKO}$ mice. Perivascular cell staining (PDGFRβ, red in **D**) and endothelial cell staining (CD31, red in **E**) of kidneys at baseline in $Sphk2^{PVCWT}$ and $Sphk2^{PVCKO}$ mice (8-12 weeks of age). Auto: autofluorescence (green). Scale bars: 100 μm.

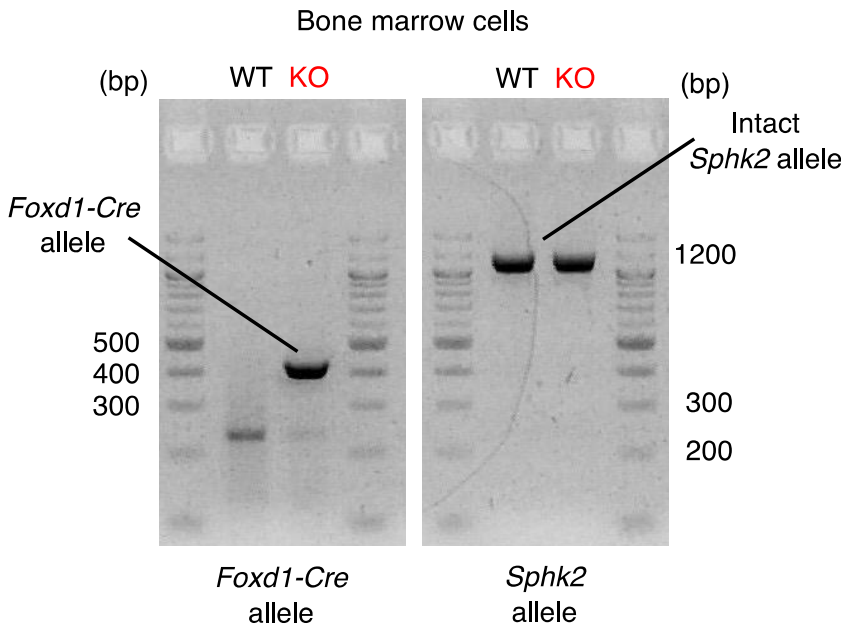

Figure S3. Cre recombination does not occur in the bone marrow cells of *Sphk2*^{PVCKO} mice. Genotyping of *Foxd1-Cre* and floxed *Sphk2* alleles. Agarose gel analysis of PCR products amplified from the DNA isolated from bone marrow cells of *Sphk2*^{PVCKO} mice (KO) and Cre-negative littermate control mice (*Sphk2*^{PVCWT}, WT). Intact *Sphk2* allele = 1220 bp, truncated *Sphk2* allele = 203 bp (cut by Cre recombinase), *Foxd1-Cre* allele = 450 bp. Note that there is no truncated *Sphk2* allele observed in the KO bone marrow cells.

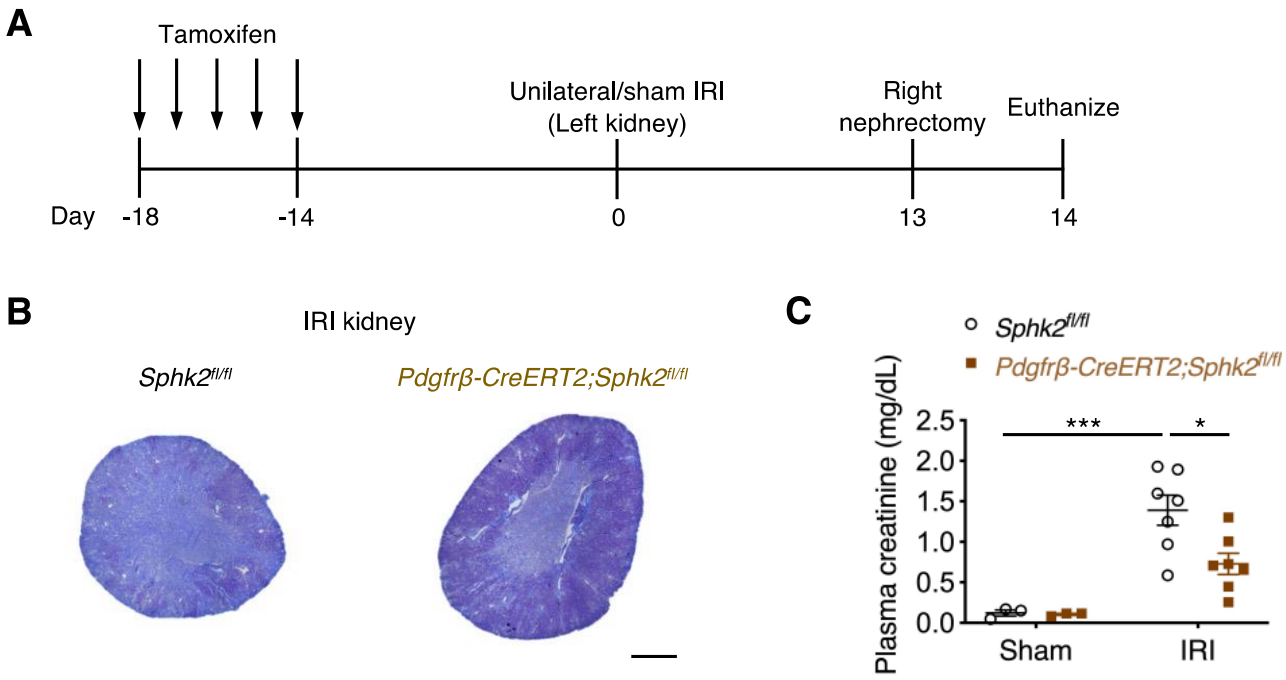

Figure S4. *Pdgfrβ-CreERT2;Sphk2$^{fl/fl}$* mice show amelioration of kidney fibrosis. (**A**) Protocol for unilateral IRI to induce kidney fibrosis (for **B** and **C**). *Pdgfrβ-CreERT2;Sphk2$^{fl/fl}$* mice and Cre-negative littermate control (*Sphk2$^{fl/fl}$*) mice received tamoxifen injection for 5 consecutive days (day -18 ~ day -14), underwent left renal pedicle clamp for 26 min (day 0) and right nephrectomy at day 13, and were euthanized at day 14. (**B**) Representative Masson's trichrome staining of collagen in IRI kidney sections at day 14. (**C**) Plasma creatinine concentrations at day 14. Scale bar: 1 mm. n = 3-7 per group. Data are represented as mean ± SEM. *$P < 0.05$, ***$P < 0.001$; two-way ANOVA followed by post hoc multiple-comparison test (Tukey's).

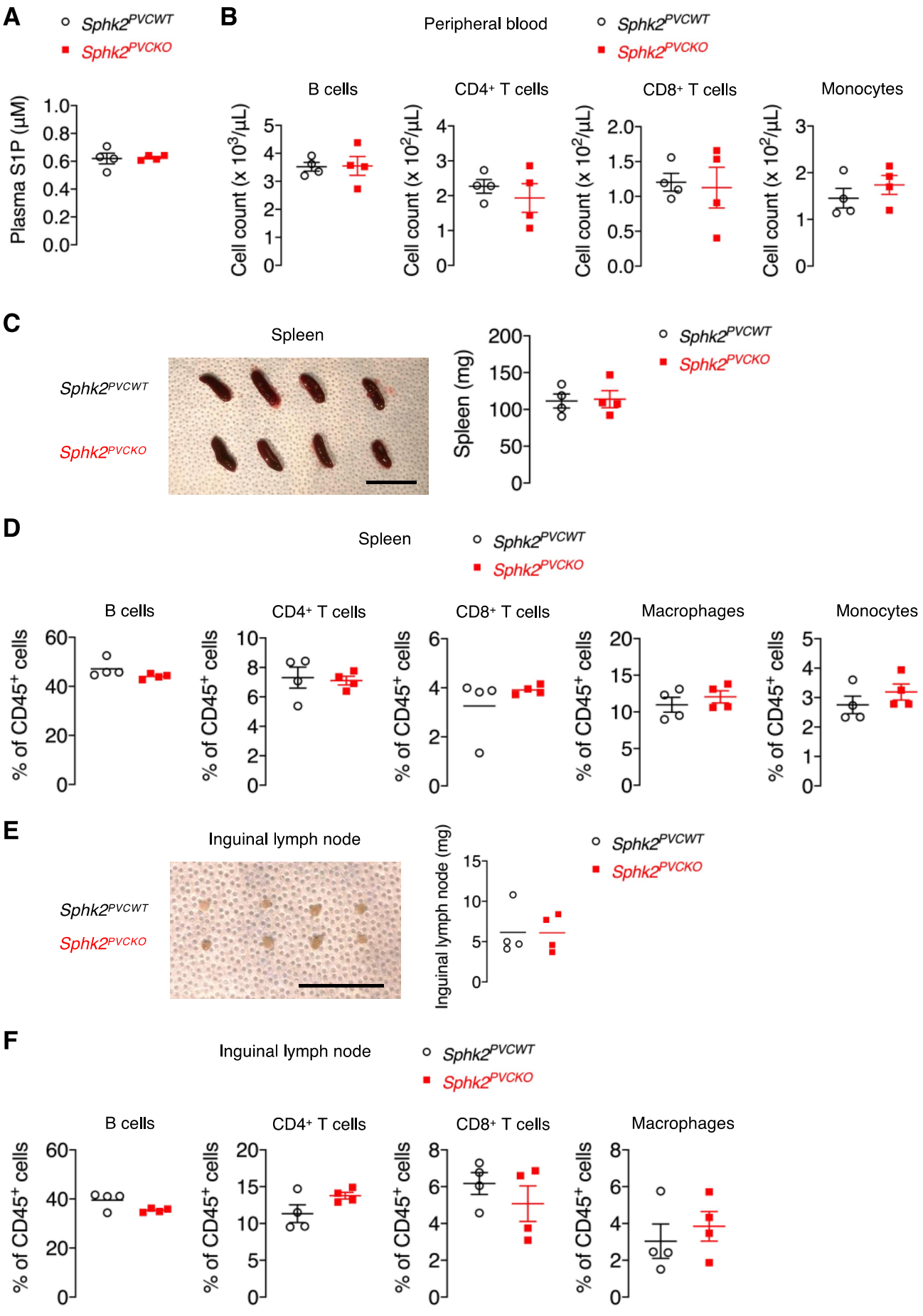
A
Sphk2PVCWT
Sphk2PVCKO
Plasma S1P (μM)
1.0
0.8
0.6
0.4
0.2
0.0
B
Peripheral blood
Sphk2PVCWT
Sphk2PVCKO
B cells
CD4+ T cells
CD8+ T cells
Monocytes
Cell count (x 10³/μL)
Cell count (x 10²/μL)
C
Spleen
Sphk2PVCWT
Sphk2PVCKO
Spleen (mg)
200
150
100
50
0
D
Spleen
Sphk2PVCWT
Sphk2PVCKO
B cells
CD4+ T cells
CD8+ T cells
Macrophages
Monocytes
% of CD45+ cells
E
Inguinal lymph node
Sphk2PVCWT
Sphk2PVCKO
Inguinal lymph node (mg)
F
Inguinal lymph node
Sphk2PVCWT
Sphk2PVCKO
B cells
CD4+ T cells
CD8+ T cells
Macrophages
% of CD45+ cells

Figure S5. Plasma S1P and immune cells in circulation and secondary lymphoid tissues are not altered in *Sphk2*^{PVCKO} mice at baseline. (**A to F**) Data from *Sphk2*^{PVCWT} and *Sphk2*^{PVCKO} mice at baseline. Plasma S1P concentrations (**A**) and the number of B cells, $CD4^+$/$CD8^+$ T cells, and monocytes in peripheral blood (**B**). (**C** and **E**) Images and weight of the spleen (**C**) and inguinal lymph nodes (**E**). (**D**) Percentage of B cells, $CD4^+$/$CD8^+$ T cells, macrophages, and monocytes in $CD45^+$ cells in the spleen. (**F**) Percentage of B cells, $CD4^+$/$CD8^+$ T cells, and macrophages in $CD45^+$ cells in inguinal lymph nodes. Scale bars: 2 cm (**C** and **E**). *n* = 4 per group. Data are represented as mean ± SEM. When no error bar is shown, this is because the data were not normally distributed and a non-parametric test was used. Data were analyzed by unpaired two-sided Student's *t* test or two-sided Mann-Whitney test.

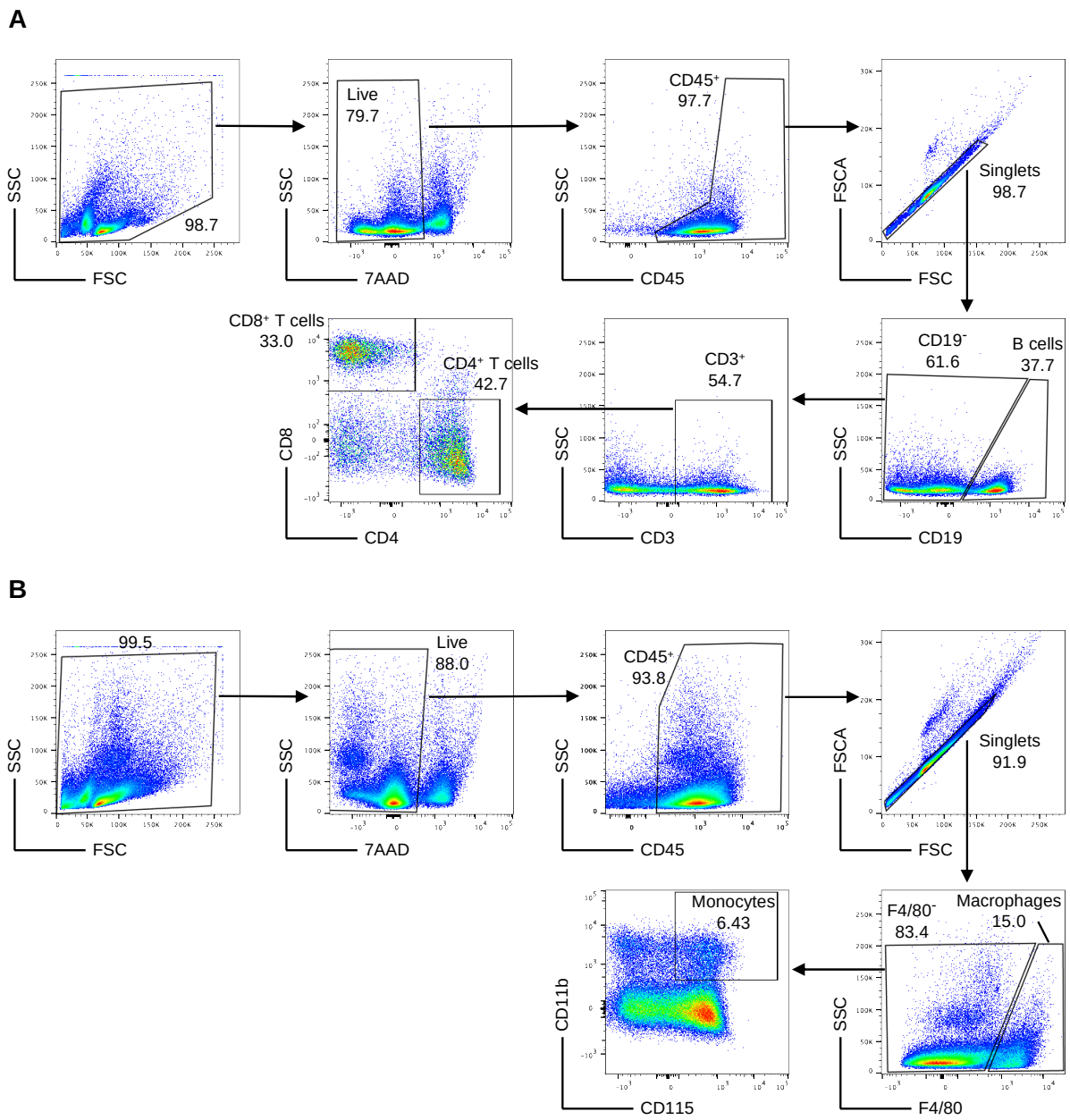

Figure S6. Gating strategy for lymphocytes, macrophages, and monocytes in circulation and secondary lymphoid tissues. (**A**) Gating strategy for lymphocytes (B cells, $CD4^+$ T cells, and $CD8^+$ T cells). Data of lymph nodes is shown as an example. After gating on live singlet $CD45^+$ cells, $CD19^+$ cells were defined as B cells, and $CD19^-/CD3^+$ cells were further divided into $CD4^+$ T cells and $CD8^+$ T cells. (**B**) Gating strategy for macrophages and monocytes. Data of the spleen is shown as an example. After gating on live singlet $CD45^+$ cells, $F4/80^+$ cells were defined as macrophages, and in the $F4/80^-$ cells, CD115 and CD11b double positive cells were defined as monocytes. Numbers on each panel indicate percent of gated population in each panel.

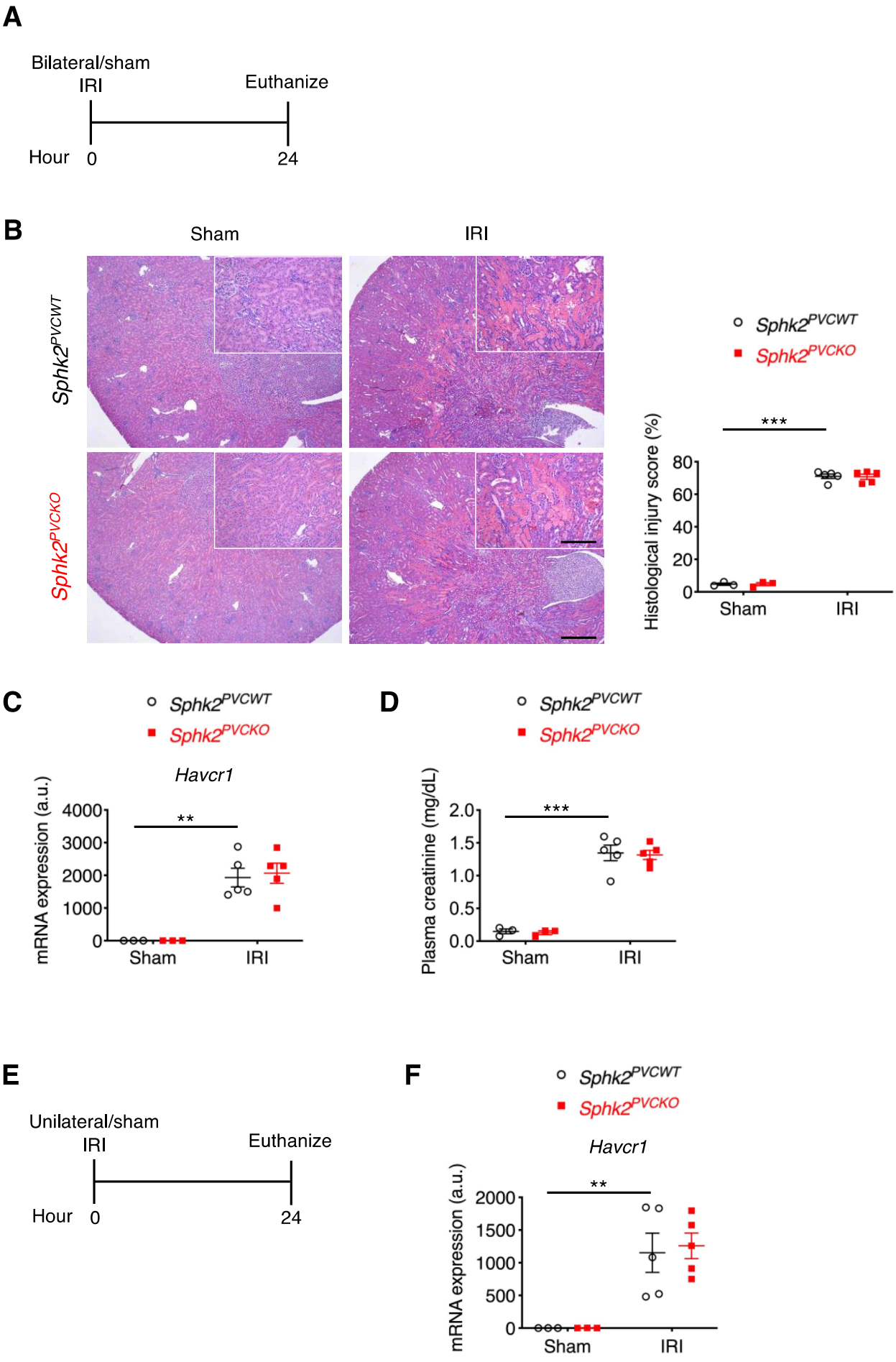
A
Bilateral/sham IRI
Euthanize
Hour 0
24
B
Sham
IRI
Sphk2PVCWT
Sphk2PVCKO
Sphk2PVCWT
Sphk2PVCKO
***
Histological injury score (%)
80
60
40
20
0
Sham
IRI
C
Sphk2PVCWT
Sphk2PVCKO
Havcr1
**
mRNA expression (a.u.)
4000
3000
2000
1000
0
Sham
IRI
D
Sphk2PVCWT
Sphk2PVCKO
***
Plasma creatinine (mg/dL)
2.0
1.5
1.0
0.5
0.0
Sham
IRI
E
Unilateral/sham IRI
Euthanize
Hour 0
24
F
Sphk2PVCWT
Sphk2PVCKO
Havcr1
**
mRNA expression (a.u.)
2000
1500
1000
500
0
Sham
IRI

Figure S7. *Sphk2* deletion in renal perivascular cells does not affect acute kidney injury in the bilateral IRI mouse model. (**A**) Protocol for bilateral IRI to induce acute kidney injury (for **B to D**). *Sphk2*^{PVCWT} and *Sphk2*^{PVCKO} mice underwent renal pedicle clamp bilaterally for 30 min, followed by reperfusion for 24 hours. (**B**) Representative H&E staining of kidney sections (left) and stereological quantification (right) of renal injury at 24 hours expressed as a percentage of the total surface area of kidney section. The inset shows the corticomedullary junction. (**C**) *Havcr1* (Kim-1) transcript expression (from whole kidney) at 24 hours. (**D**) Plasma creatinine concentrations 24 hours after bilateral IRI. (**E**) Protocol for unilateral kidney IRI to investigate the extent of acute injury (for **F**). *Sphk2*^{PVCWT} and *Sphk2*^{PVCKO} mice underwent left renal pedicle clamp for 30 min and were euthanized at 24 hours. (**F**) *Havcr1* (Kim-1) transcript expression (from whole kidney) at 24 hours. Scale bars: 400 μm; 200 μm (inset) (**B**). n = 3-5 per group. Data are represented as mean ± SEM. $^{**}P < 0.01$, $^{***}P < 0.001$; two-way ANOVA followed by post hoc multiple-comparison test (Tukey's).

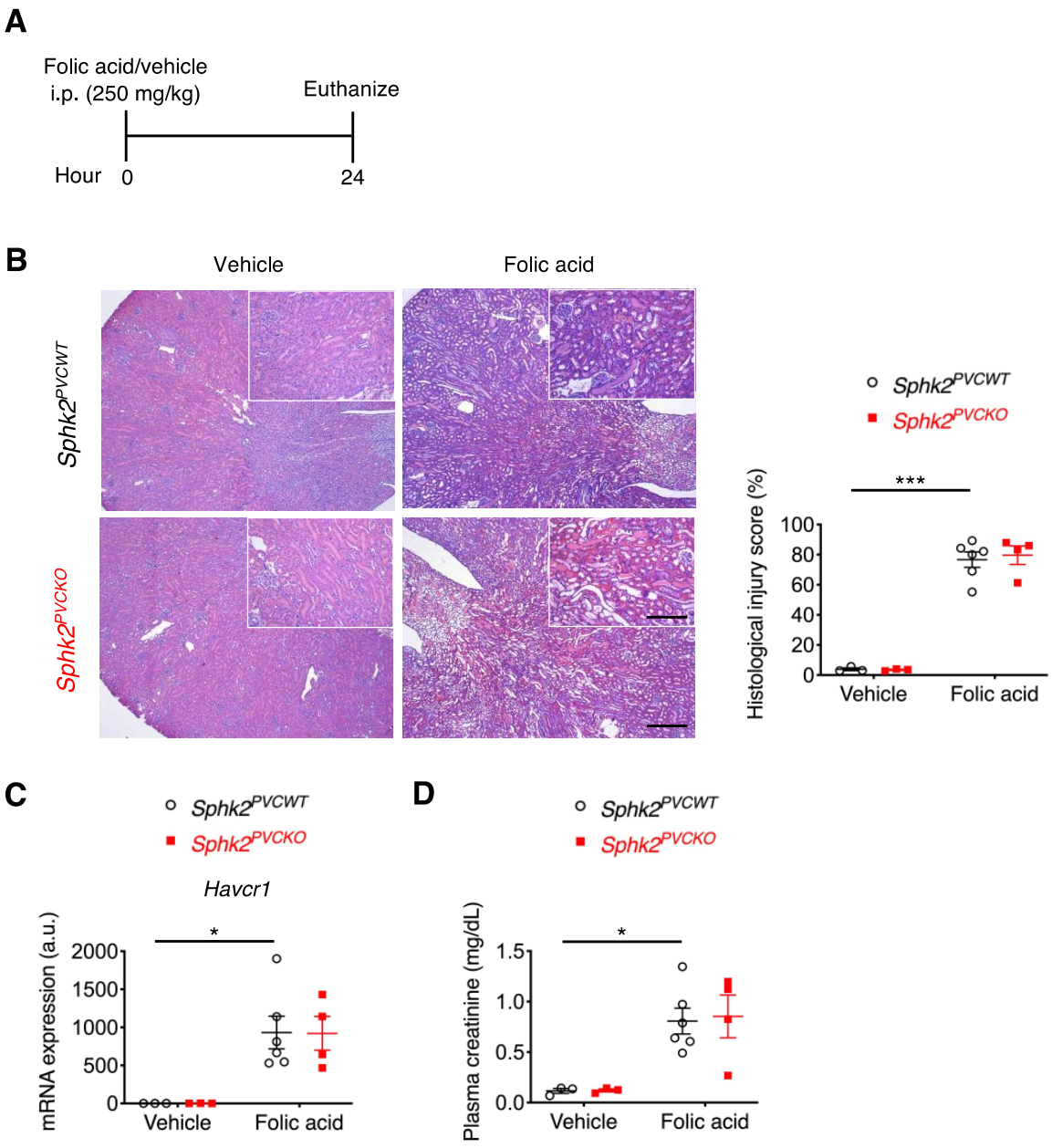

Figure S8. *Sphk2* deletion in renal perivascular cells does not affect acute kidney injury in the folic acid mouse model. (**A**) Protocol for inducing acute kidney injury by injecting folic acid (for **B** to **D**). *Sphk2*^{PVCWT} and *Sphk2*^{PVCKO} mice were given folic acid (250 mg/kg, i.p.) and euthanized at 24 hours. (**B**) Representative H&E staining of kidney sections (left) and stereological quantification (right) of renal injury at 24 hours expressed as a percentage of the total surface area of kidney section. The inset shows the corticomedullary junction. (**C**) *Havcr1* (Kim-1) transcript expression (from whole kidney) at 24 hours. (**D**) Plasma creatinine concentrations 24 hours after folic acid injection. Scale bars: 400 μm; 200 μm (inset) (**B**). *n* = 3-6 per group.

Data are represented as mean ± SEM. *$P < 0.05$, ***$P < 0.001$; two-way ANOVA followed by post hoc multiple-comparison test (Tukey's).

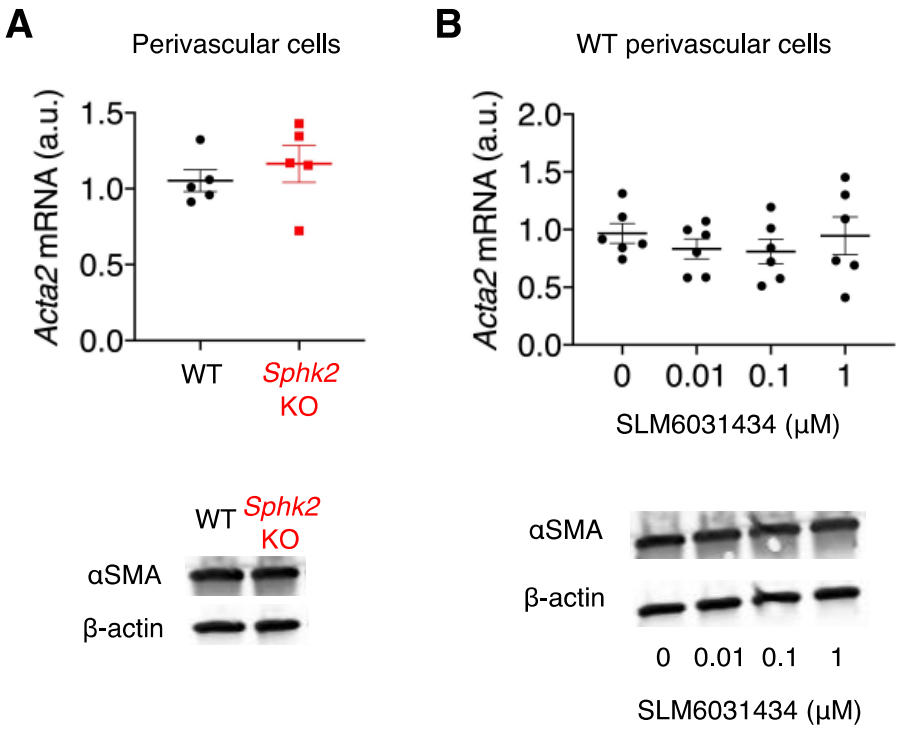

Figure S9. SphK2 inhibition does not affect transdifferentiation of perivascular cells into myofibroblasts. (**A**) Transcript (top) and protein (bottom) expression of myofibroblast marker αSMA (*Acta2*) in primary kidney perivascular cells isolated from *Sphk2*^{PVCWT} (WT) and *Sphk2*^{PVCKO} (*Sphk2* KO) mice after 24-hour TGFβ treatment. (**B**) Effect of SLM6031434 (selective SphK2 inhibitor) on αSMA mRNA (top) and protein (bottom) expression in wild-type primary kidney perivascular cells after 24-hour TGF-β treatment. $n = 5$ (**A**) or $n = 6$ (**B**) per group. Data are represented as mean ± SEM. Data were analyzed by unpaired two-sided Student's *t* test (**A**) or one-way ANOVA followed by post hoc multiple-comparison test (Tukey's) (**B**).

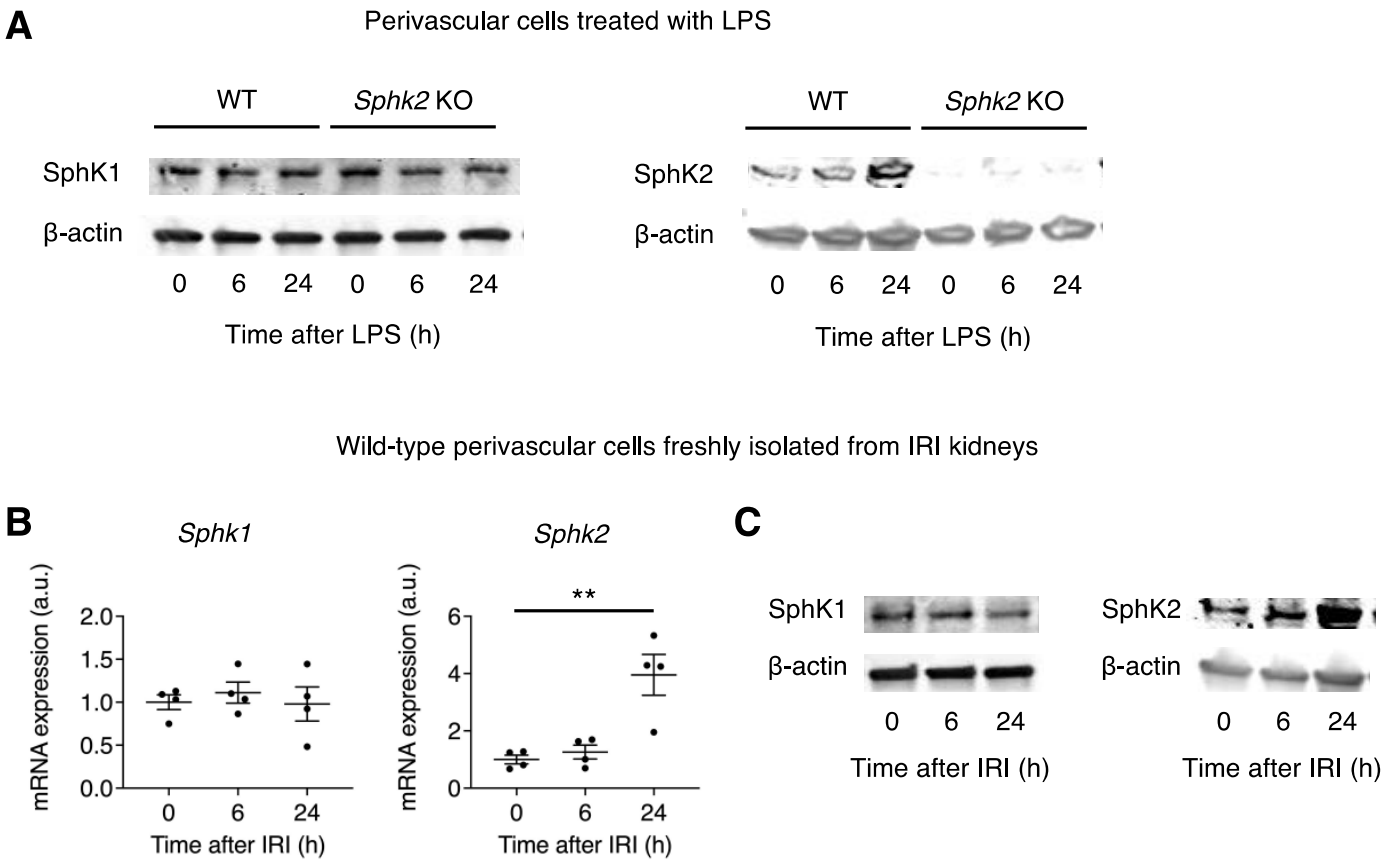

Figure S10. SphK2 but not SphK1 is upregulated in kidney perivascular cells by treatment with LPS (in vitro) or by IRI (in vivo). (**A**) Protein abundance over time of SphK1 (left) and SphK2 (right) after LPS treatment in primary kidney perivascular cells isolated from *Sphk2*^{PVCWT} (WT) and *Sphk2*^{PVCKO} (*Sphk2* KO) mice. (**B** and **C**) Time course of transcript expression (**B**) and protein (**C**) abundance of SphK1 and SphK2 in kidney perivascular cells after IRI. Wild-type (*Sphk2*^{PVCWT}) mice underwent unilateral IRI. 0, 6, or 24 hours later, kidney perivascular cells were isolated and then immediately mRNA (**B**) and protein (**C**) was extracted and analyzed. (**B** and **C**) $n = 4$ per group. Data are represented as mean ± SEM. $^{**}P < 0.01$ by one-way ANOVA followed by post hoc multiple-comparison test (Tukey's).

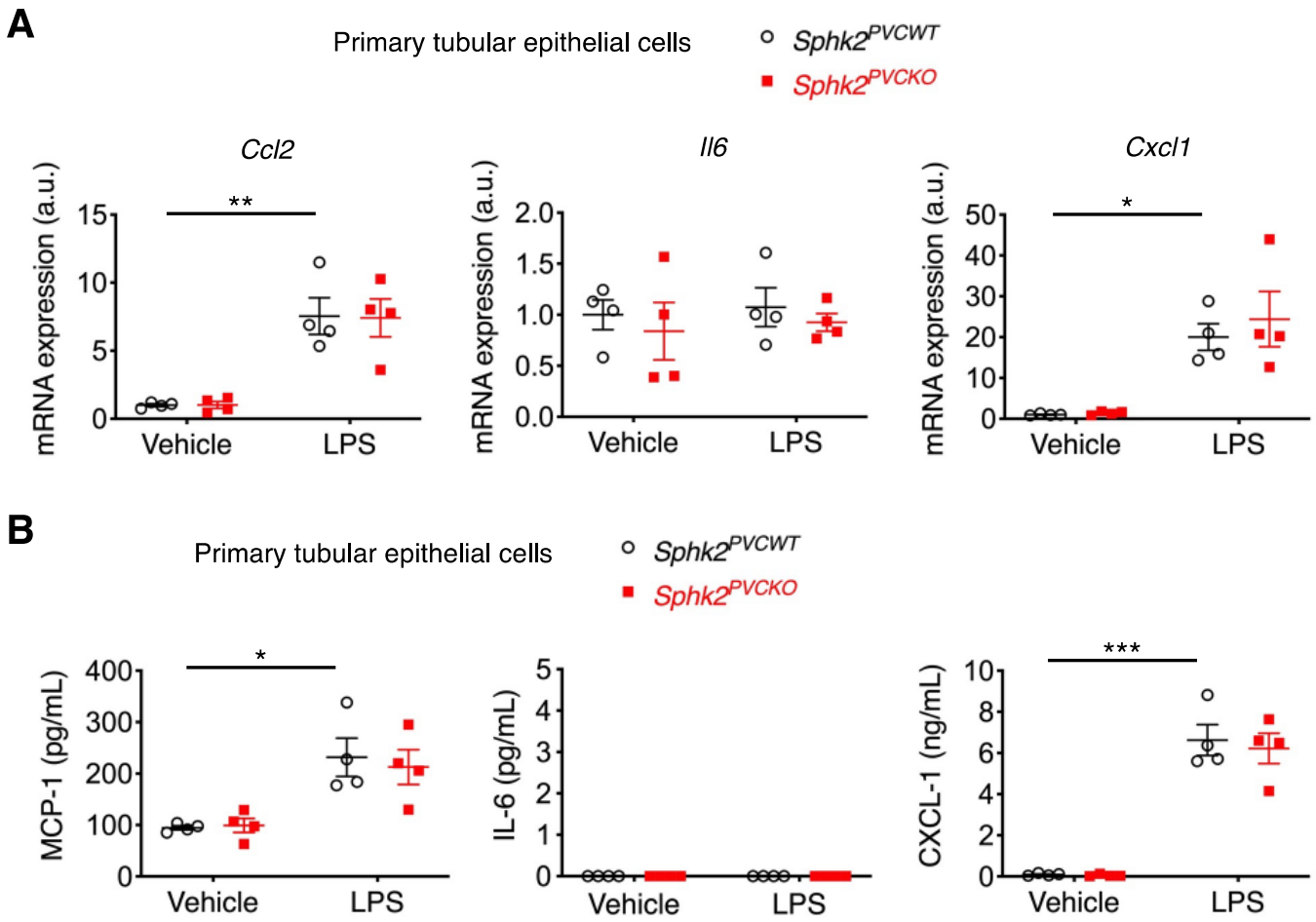

Figure S11. *Sphk2* deletion in perivascular cells does not affect inflammatory signaling in tubular epithelial cells. (**A**) *Ccl2*, *Il6*, and *Cxcl1* transcript expression 2 hours after treatment with LPS in primary tubular epithelial cells isolated from $Sphk2^{PVCWT}$ and $Sphk2^{PVCKO}$ mice. (**B**) MCP-1 and CXCL-1 (IL-6 was not detected) concentrations in supernatants of primary tubular epithelial cells treated with LPS for 24 hours. n = 4 per group. Data are represented as mean ± SEM. *$P < 0.05$, **$P < 0.01$, ***$P < 0.001$; two-way ANOVA followed by post hoc multiple-comparison test (Tukey's).

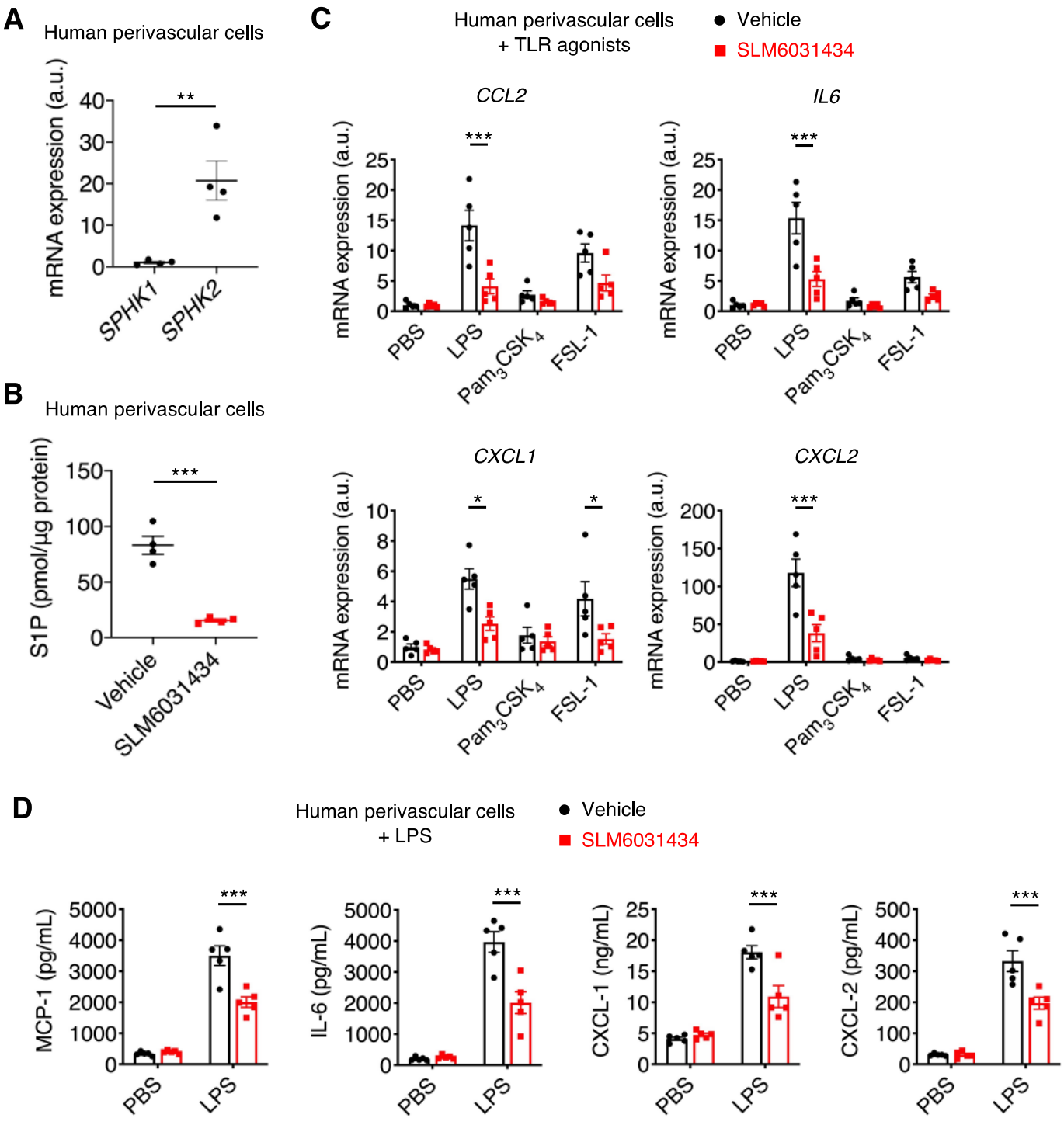

Figure S12. SPHK2 inhibition suppresses inflammatory signaling in human perivascular cells. (**A**) Baseline transcript expression of *SPHK1* and *SPHK2* in primary human kidney perivascular cells. (**B**) S1P concentrations in the supernatant of primary human kidney perivascular cells treated with 1 µM SLM6031434 (selective SPHK2 inhibitor) or vehicle (0.1% fatty acid-free BSA). (**C**) *CCL2*, *IL6*, *CXCL1*, and *CXCL2* transcript expression 2 hours after treatment with TLR2/4 agonists in primary human kidney perivascular cells.

Cells were treated with 1 μM SLM6031434 or vehicle (0.1% fatty acid-free BSA) prior to stimulation. (**D**) MCP-1, IL-6, CXCL-1, and CXCL-2 concentrations in supernatants of primary human kidney perivascular cells treated with LPS for 24 hours. Cells were treated with 1 μM SLM6031434 or vehicle (0.1% fatty acid-free BSA) prior to stimulation. $n = 4$ per group (**A** and **B**) or $n = 5$ per group (**C** and **D**). Data are represented as mean ± SEM. $^{*}P < 0.05$, $^{**}P < 0.01$, $^{***}P < 0.001$ by unpaired two-sided Student's *t* test (**A** and **B**) or two-way ANOVA followed by post hoc multiple-comparison test (Tukey's) (**C** and **D**).

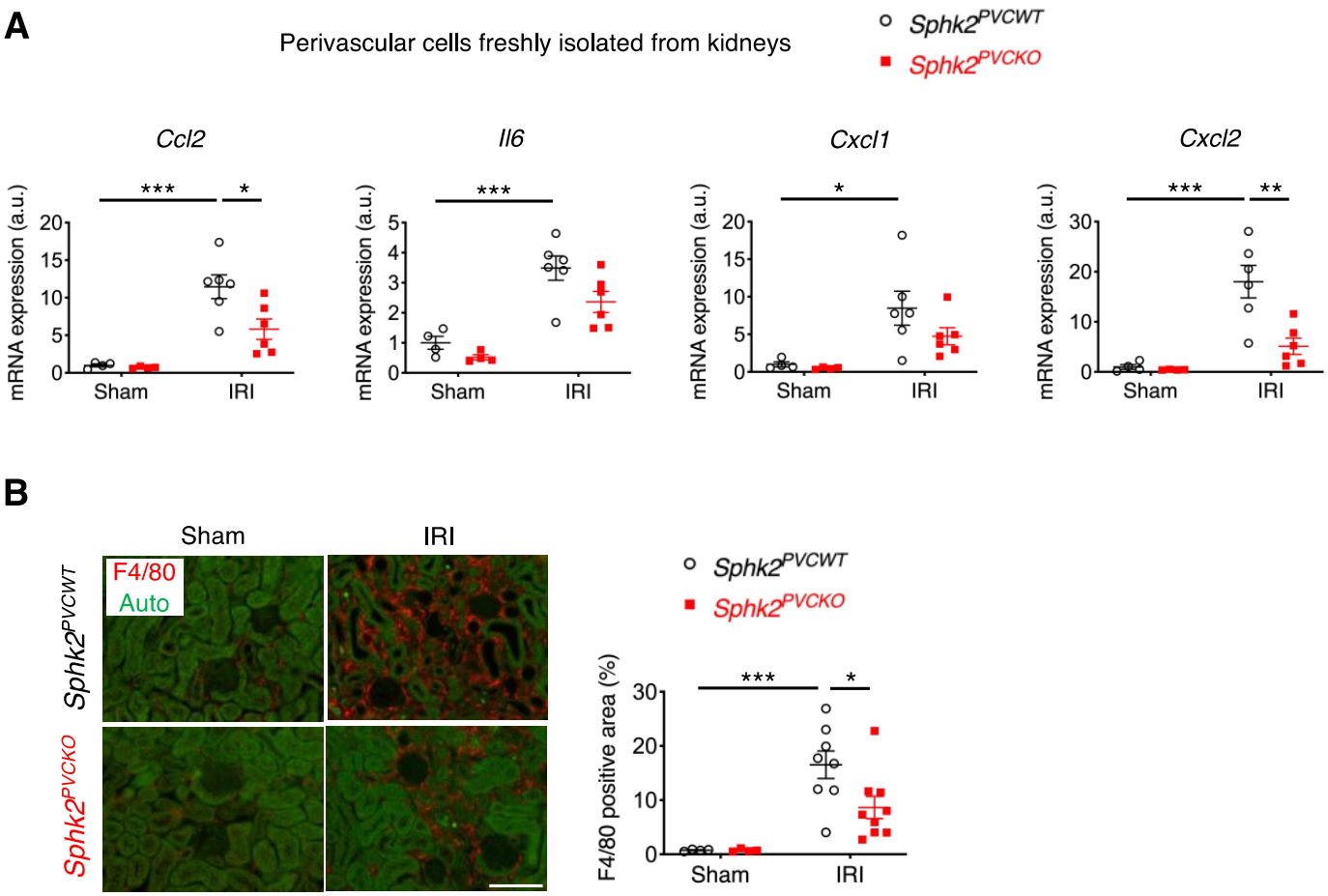

Figure S13. *Sphk2* deletion suppresses inflammatory signaling in perivascular cells in vivo and reduces macrophage infiltration in IRI mouse kidneys. (**A**) Transcript expression of proinflammatory cytokines and chemokines in kidney perivascular cells. *Sphk2*^{PVCWT} and *Sphk2*^{PVCKO} mice underwent unilateral IRI or sham, and 72 hours later kidney perivascular cells were isolated and then immediately mRNA was extracted and analyzed. (**B**) Macrophage staining (F4/80, red) of kidneys of *Sphk2*^{PVCWT} and *Sphk2*^{PVCKO} mice with quantification of F4/80 positive area as a percentage of the total surface area of kidney section at day 14 in the unilateral IRI mouse model. Auto: autofluorescence (green). Scale bar: 100 μm. $n = 4$ (sham) or $n = 6$ (IRI) per group (**A**) or $n = 4$-9 per group (**B**). Data are represented as mean ± SEM. *$P < 0.05$, **$P < 0.01$, ***$P < 0.001$; two-way ANOVA followed by post hoc multiple-comparison test (Tukey's).

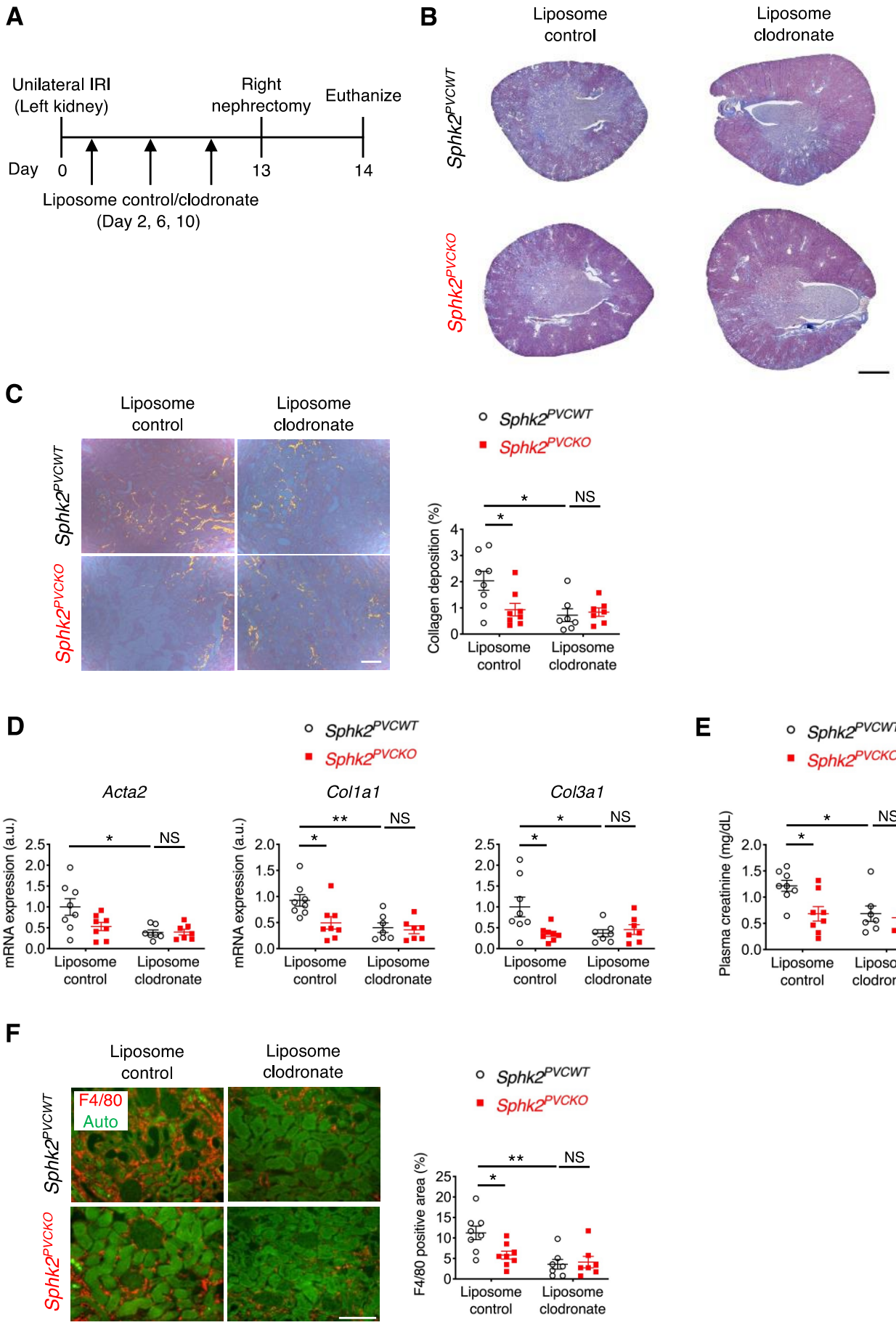
A
Unilateral IRI
(Left kidney)
Right
nephrectomy
Euthanize
Day
0
13
14
Liposome control/clodronate
(Day 2, 6, 10)
B
Liposome
control
Liposome
clodronate
Sphk2PVCWT
Sphk2PVCKO
C
Liposome
control
Liposome
clodronate
Sphk2PVCWT
Sphk2PVCKO
Collagen deposition (%)
Liposome
control
Liposome
clodronate
D
Acta2
Col1a1
Col3a1
mRNA expression (a.u.)
E
Plasma creatinine (mg/dL)
F
F4/80
Auto
F4/80 positive area (%)
NS

Figure S14. *Sphk2* deletion in perivascular cells does not further protect from kidney fibrosis in macrophage-depleted mice. (**A**) Timeline of experiments (**B** to **F**) to investigate the effect of *Sphk2* deletion in perivascular cells on kidney fibrosis in macrophage-depleted mice. $Sphk2^{PVCWT}$ and $Sphk2^{PVCKO}$ mice were administered control liposomes or liposome clodronate on days 2, 6, and 10 after unilateral IRI (200 µL on day 2 and 100 µL on days 6 and 10, i.p.), followed by right nephrectomy at day 13 and euthanasia at day 14. (**B**) Representative Masson's trichrome staining of collagen in kidney sections at day 14. (**C**) Picrosirius red staining of kidney (polarized microscopy) with quantification of red/yellow birefringence of mature collagen fibers as a percentage of the total surface area of kidney section at day 14. (**D**) *Acta2*, *Col1a1*, and *Col3a1* transcript expression (from whole kidney) at day 14. (**E**) Plasma creatinine concentrations at day 14. (**F**) Macrophage staining (F4/80, red) of kidney with quantification of F4/80 positive area as a percentage of the total surface area of kidney section at day 14. Auto: autofluorescence (green). Scale bars: 1 mm (**B**), 200 µm (**C**), and 100 µm (**F**). n = 7-8 per group. Data are represented as mean ± SEM. $^{*}P < 0.05$, $^{**}P < 0.01$; two-way ANOVA followed by post hoc multiple-comparison test (Tukey's).

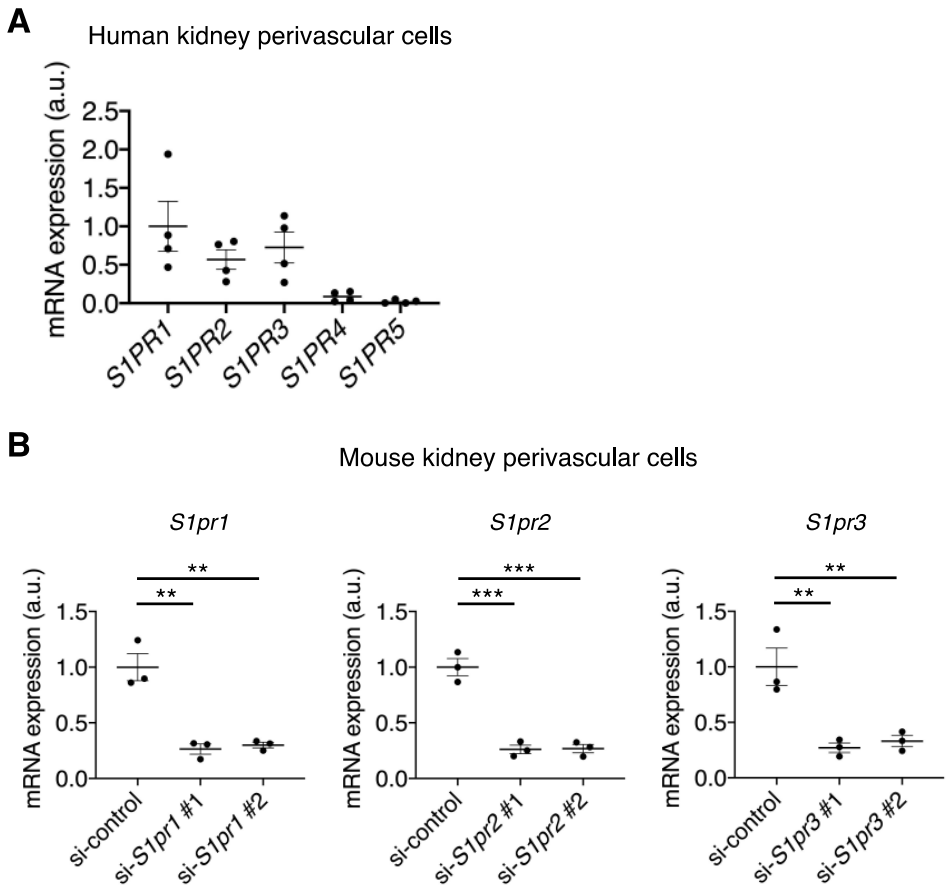

Figure S15. Expression of S1P receptors in human kidney perivascular cells and efficiency of siRNA knockdown (*S1pr1-3*) in mouse kidney perivascular cells. (**A**) *S1PR1-5* transcript expression at baseline in primary human kidney perivascular cells. (**B**) Transcript expression of *S1pr1*, *S1pr2*, and *S1pr3* in wild-type kidney perivascular cells 24 hours after siRNA transfection. $n = 4$ (**A**) or $n = 3$ (**B**) per group. Data are represented as mean ± SEM. $^{**}P < 0.01$, $^{***}P < 0.001$; one-way ANOVA followed by post hoc multiple-comparison test (Tukey's) (**B**).

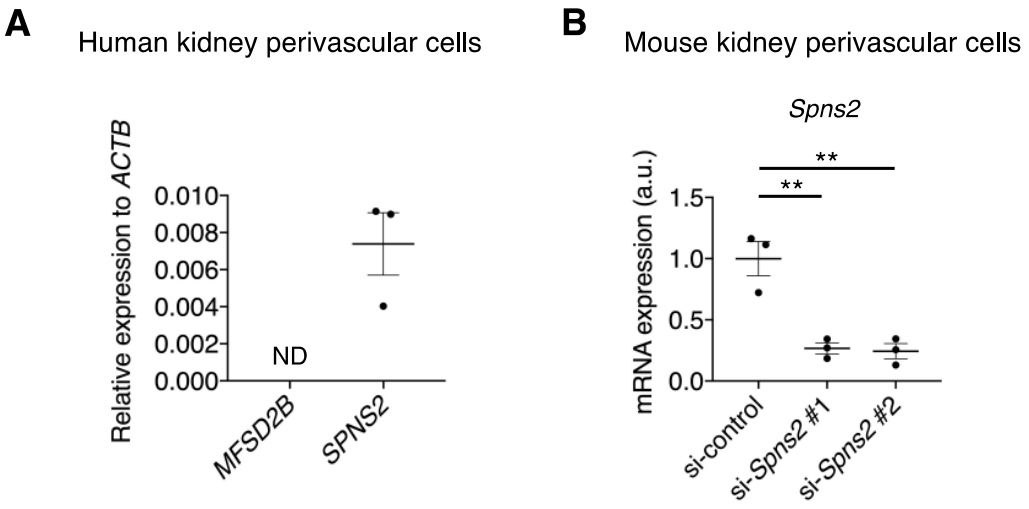

Figure S16. Expression of S1P transporters in human kidney perivascular cells and efficiency of *Spns2* siRNA knockdown in mouse kidney perivascular cells. (**A**) *MFSD2B* and *SPNS2* transcript expression at baseline in human primary kidney perivascular cells. ND, not detected. (**B**) Transcript expression of *Spns2* in wild-type kidney perivascular cells 24 hours after siRNA transfection. $n = 3$ per group (**A** and **B**). Data are represented as mean ± SEM. $^{**}P < 0.01$; one-way ANOVA followed by post hoc multiple-comparison test (Tukey's) (**B**).

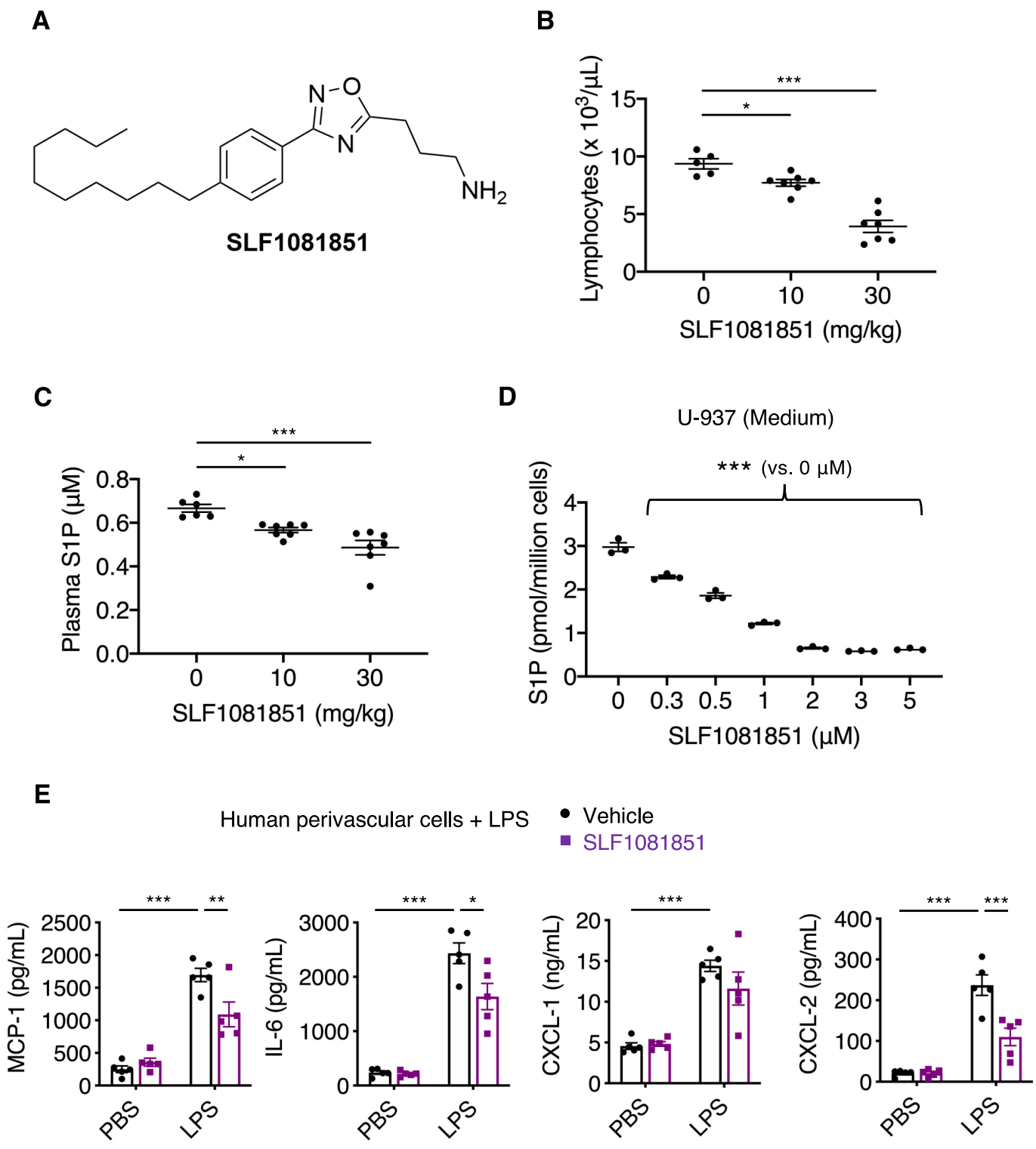

Figure S17. Characterization of the Spns2 inhibitor SLF1081851 and its effect on inflammatory signaling in human perivascular cells. (**A**) Structure of SLF1081851. (**B** and **C**) SLF1081851 was dissolved in water containing 5% hydroxypropyl-β-cyclodextrin and administered to mice (0, 10 or 30 mg/kg, i.p.). After approximately 16 hours, total lymphocyte numbers (**B**) and the amount of S1P in plasma (**C**) were examined.

(**D**) Dose response of SLF1081851 on S1P amounts in the media of human histiocytic lymphoma cells (U-937). (**E**) MCP-1, IL-6, CXCL-1, and CXCL-2 concentrations in supernatants of primary human kidney perivascular cells treated with LPS for 24 hours. Cells were treated with 3 μM SLF1081851 or vehicle (0.1% fatty acid-free BSA) prior to stimulation. n = 5-7 (**B**), n = 6-7 (**C**), n = 3 (**D**), or n = 5 (**E**) per group. Data are represented as mean ± SEM. *$P < 0.05$, **$P < 0.01$, ***$P < 0.001$ by one-way (**B**, **C**, and **D**) or two-way (**E**) ANOVA followed by post hoc multiple-comparison test (Tukey's).

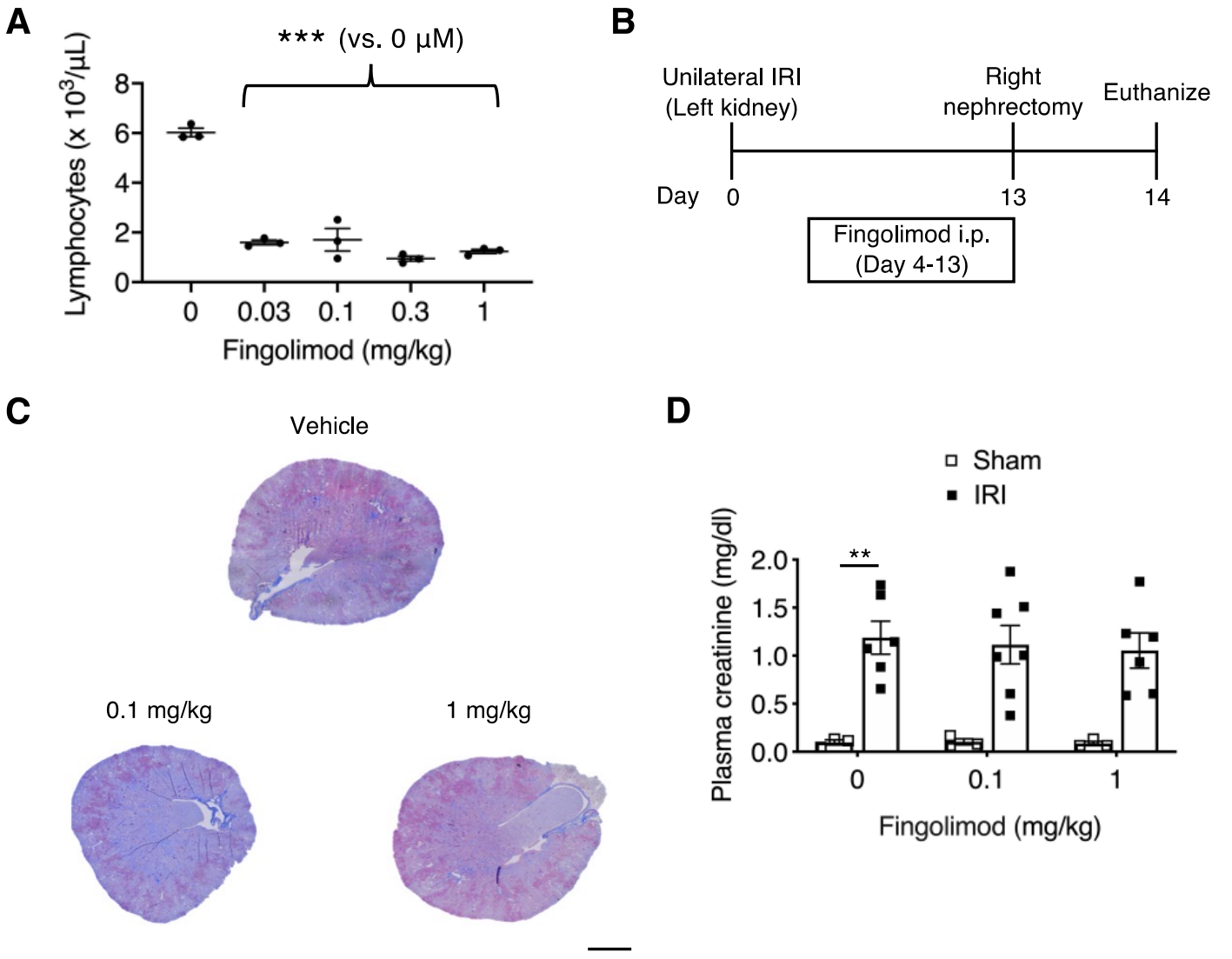

Figure S18. Fingolimod administration does not ameliorate kidney fibrosis. (**A**) Dose response of fingolimod on total lymphocyte numbers. Fingolimod was administered to mice (0, 0.03, 0.1, 0.3, 1 mg/kg, i.p.), and then after about 16 hours, total lymphocyte numbers were examined. (**B**) Timeline of experiments (**C** and **D**) to investigate the effect of fingolimod on kidney fibrosis in wild-type mice. Mice underwent unilateral IRI (day 0) and were administered fingolimod (0.1 or 1 mg/kg, i.p.) or vehicle (5% hydroxypropyl-beta-cyclodextrin) once daily from day 4 to day 13, followed by right nephrectomy at day 13 and euthanasia at day 14. (**C**) Representative Masson's trichrome staining of collagen in kidney sections at day 14. (**D**) Plasma creatinine concentrations at day 14. Scale bar: 1 mm. n = 3 (**A**) or n = 3-7 per group (**B** to **D**). Data are represented as mean ± SEM. $^{**}P < 0.01$, $^{***}P < 0.001$ by one-way (**A**) or two-way (**D**) ANOVA followed by post hoc multiple-comparison test (Tukey's).

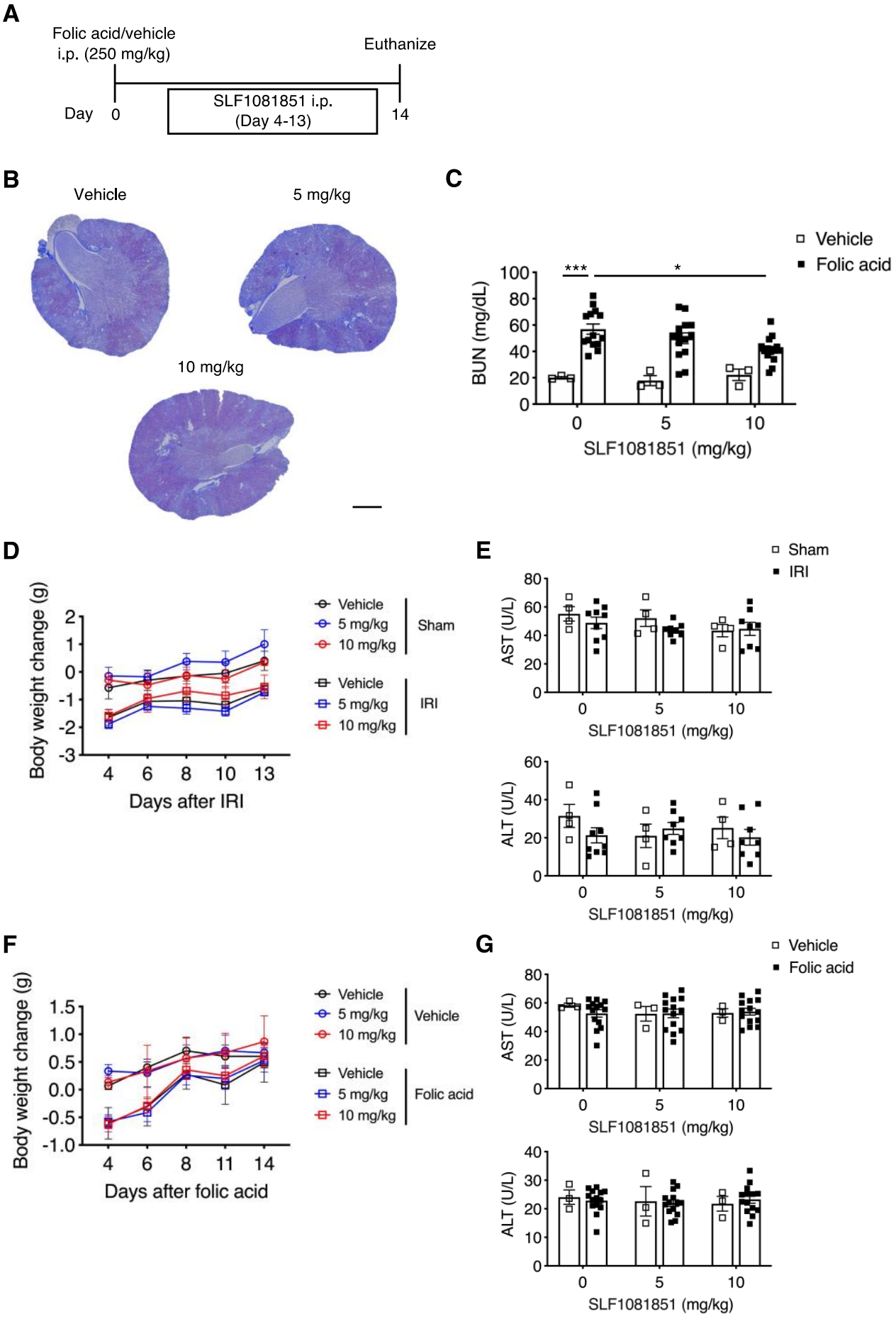
A
Folic acid/vehicle
i.p. (250 mg/kg)
Euthanize
Day 0
SLF1081851 i.p.
(Day 4-13)
14
B
Vehicle
5 mg/kg
10 mg/kg
C
Vehicle
Folic acid
BUN (mg/dL)
***
*
SLF1081851 (mg/kg)
D
Body weight change (g)
Days after IRI
Vehicle
5 mg/kg
10 mg/kg
Sham
IRI
E
Sham
IRI
AST (U/L)
ALT (U/L)
SLF1081851 (mg/kg)
F
Body weight change (g)
Days after folic acid
Vehicle
Folic acid
G
Vehicle
Folic acid
AST (U/L)
ALT (U/L)
SLF1081851 (mg/kg)

Figure S19. Pharmacological inhibition of Spns2 ameliorates kidney fibrosis in the folic acid mouse model. (**A**) Timeline of experiments (**B** and **C**) to investigate the effect of SLF1081851 on folic acid-induced kidney fibrosis in wild-type mice. Mice were given folic acid (250 mg/kg, i.p.; day 0) and were administered SLF1081851 (5 or 10 mg/kg, i.p.) or vehicle (5% hydroxypropyl-beta-cyclodextrin) once daily from day 4 to day 13, followed by euthanasia at day 14. (**B**) Representative Masson's trichrome staining of collagen in kidney sections at day 14. (**C**) Blood urea nitrogen (BUN) concentrations at day 14. (**D** to **G**) Body weight change from day 0 and plasma AST and ALT concentrations at day 14 in the unilateral IRI model (**D** and **E**; related to **Fig. 7, C to E**) and folic acid model (**F** and **G**; related to **A to C**). Scale bar: 1 mm. n = 3-14 (**A to C**, **F**, **G**) and n = 4-9 (**D** and **E**) per group. Data are represented as mean ± SEM. *$P < 0.05$, ***$P < 0.001$; two-way ANOVA followed by post hoc multiple-comparison test (Sidak's).

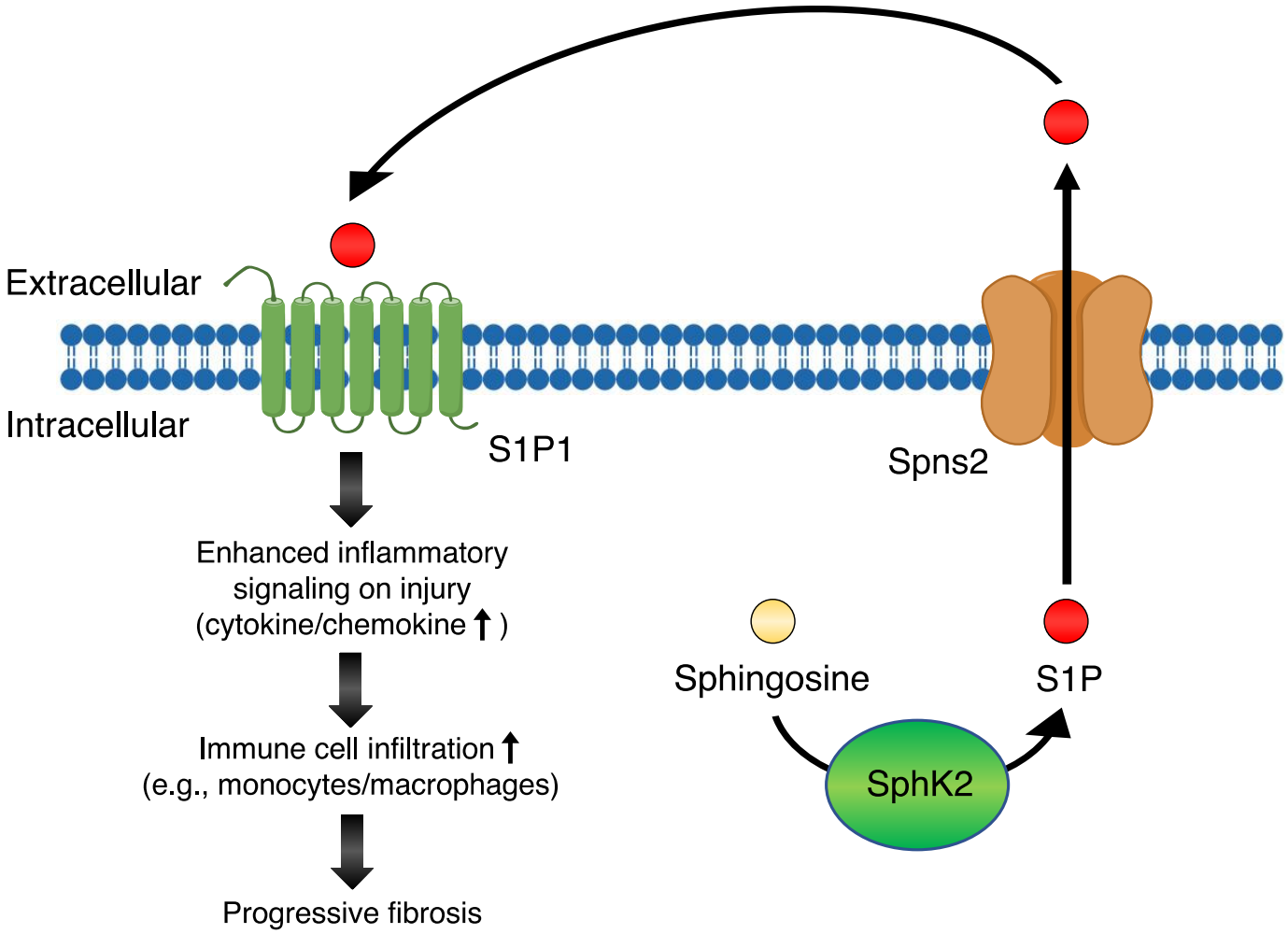

Figure S20. SphK2/S1P/Spns2/S1P1 axis enhances inflammatory signaling in kidney perivascular cells on injury, leading to immune cell infiltration and progressive fibrosis. S1P, predominantly produced by SphK2 in kidney perivascular cells, is transported into the extracellular space through Spns2 and then binds to S1P1 expressed in perivascular cells. This SphK2/S1P/Spns2/S1P1 axis enhances inflammatory signaling through production of proinflammatory cytokines and chemokines when the kidney is injured, which promotes immune cell infiltration and subsequent fibrosis. Blocking any step in this axis may be a therapeutic strategy for the prevention or treatment of kidney fibrosis.

Table S1. Primer sequences used in this study.

For genotyping

Pepck Cre	1	5'–AGGTGTAGAGAAGGCACTTAGC–3'
	2	5'–CTAATCGCCATCTTCCAGCAGG–3'
Foxd1 Cre	1	5'–TCTGGTCCAAGAATCCGAAG–3'
	2	5'–CTCCTCCGTGTCCTCGTC–3'
	3	5'–GGGAGGATTGGGAAGACAAT–3'
Pdgfrβ CreERT2	1	5'–ACATGTCCATCAGGTTCTTGC–3'
	2	5'–CCACCTTGAATGAAGTCAACAC–3'
	3	5'–AGCTTGTGGCAGTGTAGCTG–3'
S1pr1 flox	1	5'–GAGCGGAGGAAGTTAAAAGTG–3'
	2	5'–CCTCCTAAGAGATTGCAGCAA–3'
	3	5'–GATCCTAAGGCAATGTCCTAGAATGGGACA–3'
Sphk2 flox	1	5'–CTCACTGACAGGAACCCGAT–3'
	2	5'–GGAAGAGGAACGGGGAGTGA–3'
Spns2 flox	1	5'–AGCTCCCCAGCTGGTAGAAT–3'
	2	5'–AACTGACTGGCCAAGATCCC–3'

For quantitative real-time PCR

Mouse

Acta2	Fw	5'–ATTGTGCTGGACTCTGGAGATGGT–3'
	Rv	5'–TGATGTCACGGACAATCTCACGCT–3'
Actb	Fw	5'–AAGATCAAGATCATTGCTCCTCCTG–3'

	Rv	5’–AAACGCAGCTCAGTAACAGTCC–3’
Ccl2	Fw	5’–TCACCTGCTGCTACTCATTCACCA–3’
	Rv	5’–TACAGCTTCTTTGGGACACCTGCT–3’
Col1a1	Fw	5’–GAGCGGAGAGTACTGGATCG–3’
	Rv	5’–TACTCGAACGGGAATCCATC–3’
Col3a1	Fw	5’–TCCTAACCAAGGCTGCAAGATGGA–3’
	Rv	5’–ACCAGAATCTGTCCACCAGTGCTT–3’
Cxcl1	Fw	5’–TGGCTGGGATTCACCTCAAGAACA–3’
	Rv	5’–TGTGGCTATGACTTCGGTTTGGGT–3’
Cxcl2	Fw	5’–AAAGTTTGCCTTGACCCTGAAGCC–3’
	Rv	5’–TTTCCAGGTCAGTTAGCCTTGCCT–3’
Havcr1	Fw	5’–TGCTGCTACTGCTCCTTGTGAG–3’
	Rv	5’–GGCAACCACGCTTAGAGATGC–3’
Il6	Fw	5’–TGGCTAAGGACCAAGACCATCCAA–3’
	Rv	5’–AACGCACTAGGTTTGCCGAGTAGA–3’
Mfsd2b	Fw	5’–AACAAGAGCAGAAGGACGGG–3’
	Rv	5’–CCTGGAAGAACGTAGCCAGG–3’
Sphk1	Fw	5’–ACTCACCGAACGGAAGAACC–3’
	Rv	5’–GACAGCAGGTTCATGGGTGA–3’
Sphk2	Fw	5’–TTGGTCAATCCCTTTGGGGG–3’
	Rv	5’–GCCCATTCAGCACCTCGTAA–3’
Spns2	Fw	5’–GAGCCAAAGACAGCCTCATCT–3’
	Rv	5’–AGCCAATGAGGTAGGGGCTT–3’

S1pr1	Fw	5’–TTCTCATCTGCTGCTTCATCATCC–3’
	Rv	5’–GGTCCGAGAGGGCTAGGTTG–3’
S1pr2	Fw	5’–AACTCCGGGACATAGACCGA–3’
	Rv	5’–GGCTGAGCACTGGCTAGG–3’
S1pr3	Fw	5’–GCCCCTAGACGGGAGTCTTA–3’
	Rv	5’–ATAGGCTCTCGTTCTGCAAGG–3’
S1pr4	Fw	5’–CAGGCTATGCCCATTGTCCA–3’
	Rv	5’–ATCCTGAGCAACTGTGGGTG–3’
S1pr5	Fw	5’–AAATGCCCAGCTTACTCCCC–3’
	Rv	5’–GCACTGTGCAAAAGTCTCCTG–3’
Human		
ACTB	Fw	5’–ACAGAGCCTCGCCTTTGCC–3’
	Rv	5’–GCGTACAGGGATAGCACAGC–3’
CCL2	Fw	5’–TCCCAAAGAAGCTGTGATCTTCA–3’
	Rv	5’–TTTGCTTGTCCAGGTGGTCC–3’
CXCL1	Fw	5’–CGAAAAGATGCTGAACAGTGACA–3’
	Rv	5’–TTGAACTAACTTGGGGTTGACATTT–3’
CXCL2	Fw	5’–GAAAGCTTGTCTCAACCCCG–3’
	Rv	5’–TGGTCAGTTGGATTTGCCATTTT–3’
IL6	Fw	5’–CCCACCGGGAACGAAAGA–3’
	Rv	5’–TGGACCGAAGGCGCTTGT–3’
MFSD2B	Fw	5’–ACCGCCTACCGGATGACT–3’
	Rv	5’–ACTGATGCACACGGGGTAAG–3’

SPHK1	Fw	5’–CGTGGCCTCTTTGGTTTTGTTTT–3’
	Rv	5’–GTGACCTGCTCATAGCCAGCAT–3’
SPHK2	Fw	5’–GAGACCTGACTCCTTGCTCCT–3’
	Rv	5’–GGTGTCCATTCATCTGCTGGT–3’
SPNS2	Fw	5’–GAAAGTCTGAGGTGGTGCCATT–3’
	Rv	5’–CAAACCTAGGGCTGGGAACC–3’
S1PR1	Fw	5’–AGCAAGATGCGAAGCGAGC–3’
	Rv	5’–GGGGTGGTTCGATGAGTGAT–3’
S1PR2	Fw	5’–GTCCTGCACCGATTTCTCCT–3’
	Rv	5’–AGTGGTTCTGTAGTCGCACG–3’
S1PR3	Fw	5’–GACGGAGGAGCCCTTTTTCA–3’
	Rv	5’–TCCAAAATCCACGAGAGGGC–3’
S1PR4	Fw	5’–ACGTCTTTGGCTCCAACCTC–3’
	Rv	5’–CAACTTCAGATGCTCCGCAC–3’
S1PR5	Fw	5’–GGAAGCTCAGTTCACAGCCTT–3’
	Rv	5’–CCCGACAGTAGGATGTTGGC–3’

Data File S1. Raw data for all experiments where *n*<20.